



HAL
open science

Drug delivery to tumours using a novel 5-FU derivative encapsulated into lipid nanocapsules

Giovanna Lollo, Kevin Matha, Martina Bocchiardo, Jérôme Bejaud, Ilaria Marigo, Angélique Virgone-Carlotta, Thomas Dehoux, Charlotte Rivière, Jean-Paul Rieu, Stephanie Briancon, et al.

► To cite this version:

Giovanna Lollo, Kevin Matha, Martina Bocchiardo, Jérôme Bejaud, Ilaria Marigo, et al.. Drug delivery to tumours using a novel 5-FU derivative encapsulated into lipid nanocapsules. *Journal of Drug Targeting*, 2019, 27 (5-6), pp.634-645. 10.1080/1061186X.2018.1547733 . hal-02996676

HAL Id: hal-02996676

<https://hal.science/hal-02996676>

Submitted on 9 Nov 2020

HAL is a multi-disciplinary open access archive for the deposit and dissemination of scientific research documents, whether they are published or not. The documents may come from teaching and research institutions in France or abroad, or from public or private research centers.

L'archive ouverte pluridisciplinaire **HAL**, est destinée au dépôt et à la diffusion de documents scientifiques de niveau recherche, publiés ou non, émanant des établissements d'enseignement et de recherche français ou étrangers, des laboratoires publics ou privés.

1 **Drug delivery to tumors using a novel 5FU derivative encapsulated** 2 **into lipid nanocapsules**

3
4 Giovanna Lollo^{1,2*}, Kevin Matha^{2,3*}, Martina Bocchiardo², Jérôme Bejaud², Ilaria Marigo⁴, Angélique
5 Virgone-Carlotta⁵, Thomas Dehoux⁵, Rivière Charlotte⁵, Rieu Jean Paul⁵, Stéphanie Briçon¹, Olivier
6 Meyer⁶, and Jean-Pierre Benoit^{2,3}

7
8
9 1, Université de Lyon, Université Claude Bernard Lyon 1, CNRS UMR 5007, Laboratoire
10 d'Automatique et de Génie des Procédés (LAGEP), 43 bd 11 Novembre, 69622 Villeurbanne, France;
11 Institut des Sciences Pharmaceutiques et Biologiques, 8 av Rockefeller, 69373 Lyon, France.

12
13 2, MINT, Université d'Angers, INSERM U1066, CNRS UMR 6021, Angers 49933, France.

14
15 3, Pharmacy Department, Angers University Hospital, 4 rue Larrey, Angers 49933, France

16
17 4, Veneto Institute of Oncology IOV-IRCCS, 35128 Padova, Italy

18
19 5, Univ Lyon, Université Claude Bernard Lyon 1, CNRS, Institut Lumière Matière, Villeurbanne,
20 France

21
22 6, Carlina Technologies, 22 rue Roger Amsler, 49100 Angers, France

23
24 *Both authors equally contributed to the work

25 26 27 **Abstract**

28 In this work a novel lipophilic 5-FU derivative was synthesized and encapsulated into lipid nanocapsules
29 (LNC). 5-FU was modified with lauric acid to give a lipophilic mono-lauroyl-derivative (5-FU-C12,
30 MW of about 342 g/mol, yield of reaction 70%). 5-FU-12 obtained was efficiently encapsulated into
31 LNC (encapsulation efficiency above 90%) without altering the physico-chemical characteristics of
32 LNC. The encapsulation of 5-FU-C12 led to an increased stability of the drug when in contact with
33 plasma being the drug detectable until 3h following incubation. Cytotoxicity assay carried out using
34 MTS on 2D cell culture show that 5-FU-C12-loaded LNC had an enhanced cytotoxic effect on glioma
35 (9L) and human colorectal (HTC-116) cancer cell line in comparison with 5-FU or 5-FU-C12. Then,
36 HCT-116 tumor spheroids were cultivated and the reduction of spheroid volume was measured

37 following treatment with drug-loaded LNC and drugs alone. Similar reduction on spheroids volume was
38 observed following the treatment with drug-loaded LNC, 5-FU-C12 and 5-FU alone, while blank LNC
39 displayed a reduction in cell viability only at high concentration. Globally, our data suggest that the
40 encapsulation increased the activity of the 5-FU-C12. However, in depth evaluations concerning the
41 permeability of spheroids to LNC need to be performed to disclose the potential of these nanosystems
42 for cancer treatment.
43

44 1. Introduction

45 5-Fluorouracil (5-FU, 5-fluoro-1*H*,3*H*,pyrimidine-2,4-dione) is an antineoplastic agent used against a
46 wide range of solid tumors (such as breast, head and neck, colon, pancreas and stomach tumors) [1]. In
47 addition to its direct cytotoxic effect on tumor cells, the administration of low doses of 5-FU is able to
48 induce a selective depletion of immunosuppressive myeloid cell population, namely myeloid-derived
49 suppressor cells (MDSCs), which hamper tumor growth by enhancing antitumor T-cell response [2, 3].
50 Intracellularly 5-FU is converted into different cytotoxic metabolites (fluorodeoxyuridine
51 monophosphate (FdUMP), fluorodeoxyuridine triphosphate (FdUTP) and fluorouridine triphosphate
52 (FUTP). These active metabolites disrupt RNA synthesis and inhibit the action of thymidylate synthase
53 (TS). The rate-limiting enzyme in 5-FU catabolism is dihydropyrimidine dehydrogenase (DPD), which
54 converts 5-FU to its inactive metabolite dihydrofluorouracil (DHFU). More than 80% of administered
55 5-FU is normally catabolized primarily in the liver, where DPD is abundantly expressed, and as a
56 consequence lower amounts of drug are able to reach the tumor target site [1]. Moreover, lacks in drug
57 efficiency are caused by a non-favorable pharmacokinetic profile (i.e. poor distribution to the tumor
58 tissue, short plasma half-life (15-20 min), rapid catabolism, schedule-dependent toxicity profile) and
59 phenomenon of drug resistance (accelerated efflux of the active form by P-gp protein at the surface of
60 cells variation in DPD activity or gene amplification of TS) that occur frequently [4]. Additionally, 10–
61 20% of patients treated with standard 5-FU usually show severe toxicities. DPD deficiency, a
62 pharmacogenetic syndrome leading to limited detoxification capabilities, makes patients overexposed
63 and prone to toxicities, thus often hampering treatment completion, when not directly life-threatening
64 [5].

65 In this respect, to improve toxicity/efficacy balance [6] numerous modifications of the 5-FU structure
66 have been performed and novel derivatives of 5-FU have been reported [7, 8]. Among them, tegafur,
67 carmofur and floxuridine, 5-FU prodrugs, have proven their clinical efficacy with low toxicity and
68 enhanced metabolic stability [9]. Also, capecitabine (Xeloda®), an oral fluoropyrimidine carbamate,
69 that is activated selectively by the thymidine phosphorylase (TP) to form 5-FU, has been developed to
70 increase tumor selectivity [10]. However, the results obtained using these derivatives are still marginal
71 and 5FU biodistribution and toxicity remain a challenging issue in oncology.

72 Strategies based on nano and micro medicines appear as a novel therapeutic approaches to optimize drug
73 biodistribution and antitumor effect [11, 12] [13]. The final aim is to design systems with a high drug
74 loading and an optimal release of chemotherapeutic agents into the tumor tissue, which reduce drug
75 accumulation and toxicity in healthy tissues [14, 15]. A liposomal formulation named LipoFufol® made
76 of 5-FU combined to 2'-deoxyinosine and folic acid to improve its efficacy-toxicity balance has been
77 developed [16]. Besides, solid lipid nanoparticles or PLGA nanoparticles have also been described for
78 targeted delivery of 5FU [17, 18]. Even if the encapsulation in nanosystems results in an increased

79 therapeutic efficacy of the drug, its high hydrophilicity represents a limiting step for the loading of such
80 nanosystems as well as for the premature release of 5-FU from the nanocarriers when injected in blood.
81 In the present work, we combined the synthesis of a novel lipophilic 5-FU derivative made of 5-FU
82 conjugated to lauric acid and a nanotechnology approach based on lipid nanocapsules (LNC). The
83 rationale behind this strategy is that, increasing the lipophilicity of the drug, it will be possible to obtain
84 a higher drug loading and a better controlled release of the drug once encapsulated into the lipid
85 nanocarriers. The feasibility and transposability of the system were evaluated and the batch formulation
86 was scaled up 20-fold. *In vitro* studies on glioma (9L) and colon (HCT-116) cancer cell lines to assess
87 the efficacy of the derivative both in its free form or encapsulated into LNC were performed. Besides,
88 three-dimensional (3D) spheroids made of HCT-116 cells were generated and the effect of 5-FU
89 derivative alone and loaded into LNC was studied.
90 Globally, the approach presented in this paper was focused on the development of a novel 5-FU
91 derivative-loaded LNC and on the development of a more predictive *in vitro* models to highlight the
92 added value of nano-therapeutic strategies.

93

94 1. Materials and Methods

95 1.1 Chemicals

96 5-Fluorouracil (5-FU), formaldehyde, 4-dimethylaminopyridine (DMAP), *N,N'*
97 dicyclohexylcarbodiimide (DCC), lauric acid were purchased from Sigma-Aldrich (St. Quentin-
98 Fallavier, France). Acetonitrile, methanol and ethyl acetate were purchased from Fisher Scientific
99 (Illkirch, France) and silica gel from Merck (Fontenay-sous-Bois, France). Labrafac® (glyceryl
100 tricaprylate), Span 80® (sorbitane monooleate) and Kolliphor® HS 15 (polyethyleneglycol mono- and
101 di-esters of 12-hydroxystearic acid and about 30% polyethylene glycol) were obtained from Abitec
102 Corp. (Columbus, Ohio, USA), Fluka - Sigma-Aldrich and BASF (Ludwigshafen, Germany),
103 respectively; NaCl was purchased from Prolabo (Fontenay-sous-Bois, France) and water was obtained
104 from a MilliQ system (Millipore, Paris, France).

105

106 1.2 Synthesis and characterization of 5-FU-C12 derivatives

107 1.2.1 Synthesis of 5-FU-C12

108 The synthetic procedure for the preparation of 5-FU-C12 (5-fluoro-2,4-dioxo-3,4-dihydropyrimidine-
109 1(2H)-yl)methyl hexadecanoate) involved two steps and was performed according to the scheme below
110 (Figure 1).

111

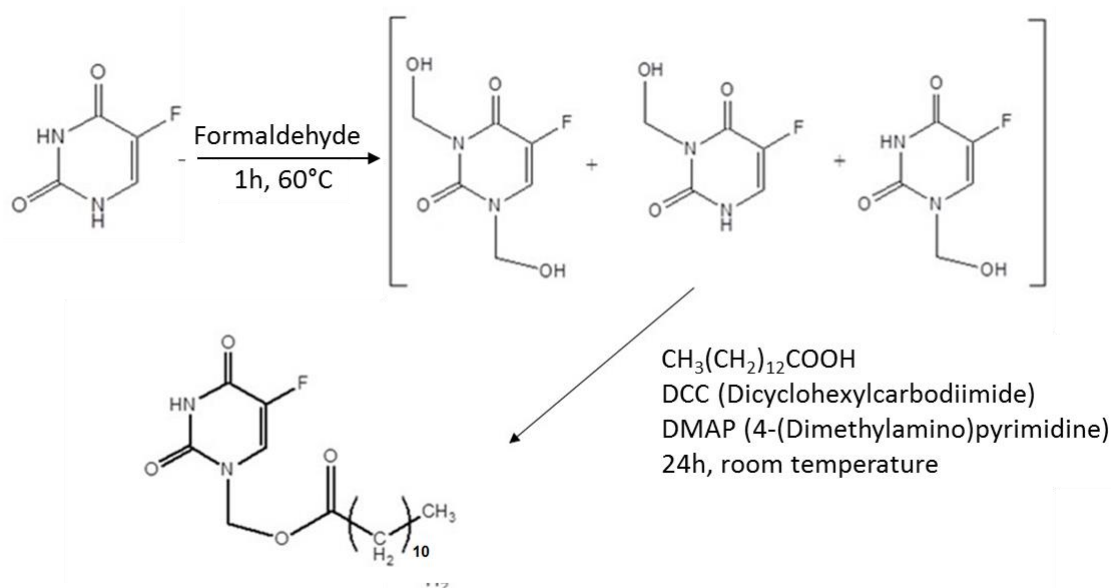


Figure 1 - Scheme of 5-FU-C12 synthesis

112
 113
 114
 115 Briefly, 5-FU (500 mg, 3.8 mmol) reacted with formaldehyde (37% wt.) in aqueous solution (50:50 v/v;
 116 2.5 mL of formaldehyde/2.5 mL of MilliQ water (Millipore, Paris, France)) in a round-bottom flask
 117 immersed in a water bath (60 °C). The reaction was conducted under magnetic stirring for 1 h and gave
 118 as products a mixture of N-1-hydroxymethyl-5-fluorouracil, N-3-hydroxymethyl-5-fluorouracil and
 119 N,N'-1,3-bis(hydroxymethyl)-5-fluorouracil [19, 20].

120 Then, the round-bottom flask was cooled in an ice-bath (0-5 °C) and acetonitrile was added (15 mL).
 121 After, DCC (1.27 g, 6.08 mmol), DMAP (34 mg, 0.266 mmol) and lauric acid (1.23 g, 6.14 mmol) were
 122 added to achieve the esterification. The reaction mixture was stirred for 1 h at 0 °C, then 24 h at room
 123 temperature and monitored by thin-layer chromatography. The secondary product dicyclohexyl urea
 124 (DCU) was separated by filtration and eliminated after several washings with acetonitrile. The product
 125 was recovered by solvent evaporation under reduced pressure and purification on a silica gel
 126 chromatographic column (isocratic elution; eluent: dichloromethane/ethyl acetate 95/5 v/v).

127
 128 **1.2.2 Characterization of 5-FU-C12: ¹H NMR**

129 Confirmation of the structure and purity of 5-FU-C12 were performed by ¹H NMR. NMR spectra were
 130 obtained on a Bruker 500 MHz spectrometer (Bruker France SAS, Wissembourg, France) using
 131 deuterated dimethyl sulfoxide (DMSO-d₆) as solvent.

132
 133 **1.2.3 Pre-formulation studies: solubility of 5-FU-C12 derivative**

134 The saturation solubility of the 5-FU-C12 derivative in different oils or solvents was determined by
 135 adding an excess amount of drug in 1 mL of various liquids in small vials. Vials were placed at room
 136 temperature or in a water bath at 60°C during 3h, and continuously stirred to reach equilibrium (48 h at
 137 25°C). After that, drug mixtures were centrifuged at 1,700 g for 20 min at 20 °C (Centrifuge Eppendorf

138 5810R - Montesson, Paris, France). The supernatant was separated and added to acetonitrile and
139 solubility was quantified by HPLC at 215 nm. The solubility studies were carried out in triplicate and
140 results were reported as mean \pm SD. LogP was also calculated through the program ACD/ChemSketch
141 (Advanced Chemistry Development (ACD/Labs), Strasbourg, France).

142

143 1.2.4 HPLC determination of 5-FU-C12

144 Chromatography was performed using a Waters 717 Plus Autosampler and a Waters 600 Pump
145 Controller (Waters S.A., Saint-Quentin-en-Yvelines, France) with an XTerra® C18- RP18 5 μ m 150
146 mm x 4.6 mm column (Waters, Milford, Ireland) with precolumn and a Waters 2487 Dual Absorbance
147 Photodiode Array Detector set at $\lambda = 263$ nm. A 40 μ L aliquot of each filtrate was injected in duplicate
148 into the HPLC column. The column was eluted at 1 mL/min flow rate using a gradient obtained by
149 mixing amounts of MilliQ water (A) and acetonitrile (B). The initial mobile-phase composition was
150 90% A and 10% B; a first linear gradient was applied to reach a composition of 70% A 30% B after 5
151 min, a second linear gradient was applied to reach a composition of 100% B after 10 min, maintained
152 for 5 min and then returned to 90% A and 10% B. The peak of 5-FU-C12 appears at 16.5 min. Data
153 acquisition, analysis and reporting were performed using Empower chromatography software (Milford,
154 Massachusetts, USA).

155

156 1.4 Preparation of blank and 5-FU-C12-loaded LNC

157 LNC were formulated using a phase inversion-based process previously described [21, 22]. Briefly,
158 different amounts of 5-FU-C12 were firstly stirred in a mixture of Labrafac® and Span® 80. Then,
159 0.967 g of Kolliphor® were added together with NaCl (45 mg) and water (1.02 mL). Three temperature
160 cycles (between 45 and 70 °C) were performed to obtain the phase inversion of the emulsion. Between
161 these temperatures, there was a phase inversion zone (PIZ) at around 55-60 °C. At 1–3 °C from the
162 beginning of the PIZ of the last temperature cycle, a rapid cooling and dilution with purified ice cooled
163 water (2.15 g) led to LNC formation. The nanocapsules were then stored at 4 °C. Sterile 5FU-C12 LNC
164 batches were obtained by filtration through 0.22 μ m Millipore® Stericup™ filter units (Merck,
165 Darmstadt, Germany). Sterility of the formulation was assessed using soybean casein digest medium at
166 20-25°C and thioglycolate medium at 30-35°C incubated during 14 days and 5 days of subculture
167 according to the Ph. Eur. 9 (Confarma, Hombourg, France). Endotoxin content was assessed using
168 chromogenic kinetic method with kinetic QCL Limulus Amebocyte Lysate in GMP conditions
169 (Confarma, Hombourg, France).

170

171 1.5 Characterization of blank and 5-FU-C12 loaded LNC

172 1.5.1 Physicochemical characterization

173 Particle size analysis and zeta potential measurements of LNC were measured using a Malvern
174 Zetasizer® apparatus DTS 1060 (Nano Series ZS, Malvern Instruments S.A., Worcestershire, UK) at
175 25 °C, in triplicate, after dilution of LNC dispersions in deionized water.

176

177 1.5.2 Cryogenic-transmission electron microscopy (cryoTEM)

178 To evaluate the morphology of blank and loaded LNC, diluted samples were dropped onto 300 Mesh
179 holey carbon films (Quantifoil R2/1) and quench-frozen in liquid ethane using a cryo-plunge
180 workstation (made at Laboratoire de Physique des Solides-LPS Orsay, France). The specimens were
181 then mounted on a precooled Gatan 626 specimen holder, transferred in the microscope (Phillips
182 CM120) and observed at an accelerating voltage of 120 kV (Centre Technologique des Microstructures
183 (CTμ), platform of the University Claude Bernard Lyon 1, Villeurbanne, France).

184

185 1.5.3 Determination of drug encapsulation efficiency

186 Firstly, the mixtures of Labrafac® and Span®80, in which 5-FU-C12 was solubilized, were collected
187 and analyzed by HPLC (after dilution 1:1000 in acetonitrile) to calculate the total amount of 5-FU-C12
188 dissolved. Once the LNC were formulated, they were filtered through a 0.2 μm filter to eliminate the
189 free drug. Samples of drug-loaded LNC were prepared by dissolving an aliquot of LNC dispersion in
190 acetonitrile (dilution 1:200) and 40 μL were injected in the HPLC according to the protocol previously
191 described. The encapsulation efficiency (%) was determined according to the following formula:

$$192 \quad EE (\%) = \frac{\text{measured drug payload}}{\text{theoretical drug payload}} \times 100$$

193

194 Linear titration curves, with freshly made 5-FU-C12 acetonitrile solutions at a concentration range from
195 0.5 to 25 μg/mL, were used to extrapolate results ($r^2 > 0.999$).

196

197 1.5.4 Storage stability studies in colloidal suspension of 5-FU-C12-loaded LNC at 4°C

198 The stability of 5-FU-C12-loaded LNC was evaluated after storage at + 4 °C during 1 month. The
199 macroscopic aspect, particle size, polydispersity and leakage of the drug were assessed at fixed time
200 intervals and after filtration using a Minisart® 0.2 μm filter (Merck, Fontenay-sous-Bois, France).

201

202 1.5.5 Stability in plasma of 5-FU-C12-loaded LNC

203 The stability in a relevant physiological medium was evaluated using human plasma provided by
204 Etablissement Français du Sang (EFS, Pays de la Loire, Nantes, France).

205 Samples of plasma were defrosted and diluted (80:20) with filtered PBS (0.22 μm filter). Thirty samples
206 were prepared mixing 50μL of 5-FU-C12-loaded LNC or 5-FU-C12 and kept at 37°C in a water bath.
207 At different time points (0, 5, 10, 15, 30, 60, 180, 360 min and 24 and 48 h), samples were taken and

208 diluted with 800 μ L of acetonitrile in order to precipitate plasma proteins and centrifuged at 12,290 g
209 during 15 min at 4°C. Supernatants were recovered, filtered through 0.22 μ m filter and analyzed by
210 HPLC as previously described. Calibration curve of 5-FUC12 in plasma from 1 to 22.5 μ g/mL was
211 performed ($r^2 > 0.999$).

212

213 1.5.6 *In vitro* release studies of 5-FU-C12-loaded LNC

214 The release rate of 5FUC12 from the loaded LNC was determined using an *in vitro* dialysis technique
215 [23]. Briefly, a known suspension of 5-FU-C12-loaded LNC was dispersed in a solution of freshly
216 prepared phosphate buffered saline (PBS), pH 7.4, containing Tween® 80 (0.1%, w/v). The mixture was
217 incubated at 37°C and subjected to continuous shaking at 100 rpm, using magnetic stirring. The released
218 5-FU-C12 was sampled at defined time periods (0.5h, 1h, 3h, 5h, 8h, 12h, 24h and 48h) . An aliquot was
219 recovered and immediately replaced with an equal volume of fresh solution. The concentration of the
220 aliquot was measured using the HPLC method previously described.

221

222 1.6 Scale-up formulation study

223 Batches of 5-FU-C12-loaded LNC were scaled up to 112 g (twenty times bigger than the lab scale). The
224 experimental conditions were adapted in order to prepare up to 100 mL of LNC in a single step process.
225 An intermediate volume (50 mL, 56g) was used in order to evaluate the robustness of the formulation
226 process. Blank and 5-FU-C12-loaded LNC were characterized in terms of mean size, zeta potential, and
227 encapsulation efficiency using the methods previously described.

228

229 1.7 *In vitro* experiments

230 1.7.1 Cell culture

231 Two cell lines have been cultured to carry out the experiments: rat 9L gliosarcoma cells and human
232 HCT-116 colorectal carcinoma cancer cell.

233 9L cells were obtained from the European 127 Collection of Cell Culture (Sigma, Saint-Quentin
234 Fallavier, France). HCT-116 colorectal carcinoma (CCL247) cell line was purchased from the American
235 Type Culture Collection (ATCC, Manassas, Virginia, USA).

236 9L cells were grown in EMEM (Lonza, Verviers, Belgium) supplemented with 10% fetal bovine serum
237 (Lonza), 1% antibiotics (10,000 units penicillin, 10 mg streptomycin, 25 μ g amphotericin B/mL
238 solubilized in appropriate citrate buffer (Sigma–Aldrich)) and 1% non-essential amino acids (Lonza).

239 HCT-116 line were cultured in DMEM-Glutamax (Lonza) supplemented with 10% of heat-inactivated
240 fetal bovine serum (FBS; Sigma, St. Louis, Missouri, USA), 100 units/100 μ g of penicillin/streptomycin.
241 Cell lines (9L and HCT-116) were thawed and cultured in T75 flasks with filter caps (Thermo
242 Scientific™ Nunc™, Villebon-sur-Yvette, France), maintained at 37 °C in a humidified atmosphere
243 with 5% of CO₂.

244

245 1.7.2 *In vitro* cell viability

246 *In vitro* cytotoxicity assays were performed using CellTiter 96® AQueous One Solution cell
247 proliferation assay kit (Promega, Charbonnières-Les-Bains, France) containing a tetrazolium compound
248 [3-(4,5-dimethylthiazol-2-yl)-5-(3-carboxymethoxyphenyl)-2-(4-sulfophenyl)-2H-tetrazolium, inner
249 salt; MTS]. Briefly, 9L (6,950×10³ per well) and HT-116 cells (3,500×10³ per well) were plated into
250 96-well plates and incubated at 37°C during 48h in air controlled atmosphere (5% CO₂). The medium
251 was removed and cells were treated during 48h with increasing concentrations 5-FU-C12 LNC diluted
252 with serum free DMEM medium supplemented with 1% antibiotics (10,000 units penicillin, 10 mg
253 streptomycin, 25 µg amphotericin B/mL solubilized in appropriate citrate buffer), 1% HEPES buffer,
254 1% NEAA (Non Essential Amino Acid) 100X (Lonza), 1% sodium pyruvate (Lonza), 1% N1 medium
255 supplement 100X (0.5 mg/mL recombinant human insulin, 0.5 mg/mL, human transferrin partially iron-
256 saturated, 0.5 µg/mL sodium selenite, 1.6 mg/mL putrescine, and 0.73 µg/mL progesterone (Sigma-
257 Aldrich)).

258 After incubation for 48h, cell survival percentage was determined using the CellTiter 96® AQueous
259 One Solution cell proliferation assay kit. According to the procedure described by the supplier, medium
260 with treatments was removed and 200 µL of a 1:5 diluted MTS solution were added in each well. After
261 2 h at 37 °C, the absorbance at 492 nm was recorded using a Microplater Reader (Multiskan Ascent®,
262 Labsystem, Cergy Pontoise, France).

263 Cell viability (CV) percentage was evaluated through the following formula:

$$264 \quad CV (\%) = \frac{\text{Absorbance treated well}}{\text{Absorbance control well}} \times 100$$

265
266 with *Absorbance control* well, the absorbance value of untreated cells (incubated only with fresh
267 medium).

268

270 1.7.3 Dose response curves of *in vitro* cell viability data and IC₅₀

271 Dose (concentration of drug treatments, µM) response (cellular viability, %) curves were plotted for the
272 test after correction by subtracting the background (medium) absorbance. Percentage of viable cells was
273 calculated based on the absorbance values (λ = 492 nm) in cells treated with media only (assumed as
274 100% viable). A linear model was used to estimate the regression parameters. In particular, the Log
275 transformation of concentration used was calculated in order to have a normal distribution for this
276 variable. This model allowed us to estimate the concentration of the drug required to reduce cell viability
277 by 50% (IC₅₀) and CI (confidence interval) stated at the 95% confidence level.

278

279 1.7.4 3D cell model: MCTS formation and treatment

280 Multi cellular tumor spheroids (MCTS) were formed according to a previous published method [24].
281 Briefly, MCTS were formed using HTC-116 the cell line in Ultra Low Attachment (ULA) 96 wells

282 Round-Bottom plate (Greiner bio-one) to avoid cell-substrate attachment. The cells were trypsinized
283 and were counted using a Malassez grid in order to obtain 2,400 cells per milliliter. This concentration
284 of cells (i.e., 480 cells per well in a volume of 200 μL) was chosen in order to obtain a single spheroid
285 per well, with a spheroid diameter at the end of the experimentation not exceeding 500 μm .
286 The plate was centrifuged for 5 minutes at 1,200 g at room temperature to initiate the formation of
287 spheroids. The plate was placed in the incubator under agitation at 37°C and 5% CO_2 during the whole
288 experiment. At the end of the first day after seeding, 100 μL of culture medium was added to ensure
289 proper 3D growth. After two days after seeding, MCTS were treated with 5-FU aqueous solution, 5-FU-
290 C12 diluted in acetone and 5-FU-C12-loaded LNC at various drug concentrations: 2, 10 and 50 μM .
291 Blank LNC were also used to assess nonspecific toxicity that could arise from the system. MCTS were
292 monitored at 24 and 48h post treatment. Eight spheroids ($n=8$) were probed at each concentration. A
293 ring of detaching cells appeared spontaneously after one day of treatment. The spheroids were
294 transferred into new well plates to eliminate mechanically this uncohesive peripheral cell layer and to
295 renew the drug and culture medium. Therefore, the reduction in volume we monitor during the therapy
296 (see section 1.7.6) arises from a loss of viability as well as from a loss of cohesiveness.

297

298 1.7.6 Phase contrast follow up of MCTS volume

299 Photographs of MCTS were taken with an inverted microscope (Leica DMIRB) in phase contrast inside
300 the 96-well plates at 0, 24 and 48h time points after 5-FU exposure. We performed edge detection using
301 a sobel threshold for each spheroid using the ImageJ software. The resulting binary images were fitted
302 to an ellipse of major (L_M) and minor (L_m) axes using the ImageJ “Analyse Particles” plugins. From
303 this, a mean diameter was calculated, $D = (L_M + L_m)/2$. The volume V was then determined assuming
304 that the spheroids are spherical $V = \pi D^3/6$.

305

306 1.8 Statistical analysis

307 For the results of *in vitro* cytotoxic activity evaluation, statistical differences were determined using non
308 parametric tests, such Wilcoxon-Mann-Whitney test and Kruskal-Wallis test. The type one error rate
309 was taken as $\alpha = 5\%$ ($p < 0.05$).

310

311 2. Results

312 2.1 Synthesis of 5-FU-C12

313 In order to obtain the lipophilic 5-FU derivative named 5-FU-C12 made of 5-FU conjugated to lauric
314 acid, a two-step process was performed. In the first step of the synthesis, pure 5-FU reacted with aqueous
315 formaldehyde to give a mixture of *N-NI*-bis-(hydroxymethyl-5-fluorouracil) and mono-hydroxymethyl
316 substituted 5-FU (*N-1*- hydroxymethyl-5-fluorouracil, *N-3*-hydroxymethyl-5-fluorouracil). As
317 previously described by Liu *et al.*, [19] following this step, the 1H NMR spectrum showed that *N-1*-
318 hydroxymethyl-5-fluorouracil was obtained in higher amount than the others [19]. Then, the preferential

319 conjugation of lauric acid in the N1 position by means of DCC/DMAP chemistry was achieved. The
320 alkyl chain was attached in preference to the functionalized nitrogen in position 1 because the amount
321 of intermediate *N*-1-hydroxymethyl-5-fluorouracil was higher than the others [20] and also because this
322 was the sterically less hindered and more nucleophilic site (due to its higher pKa value). After
323 purification by silica gel column chromatography, 5-FU-C12 (molecular weight (MW) 342 g/mol) was
324 recovered as the main product in the form of white powder with a yield of 70%.

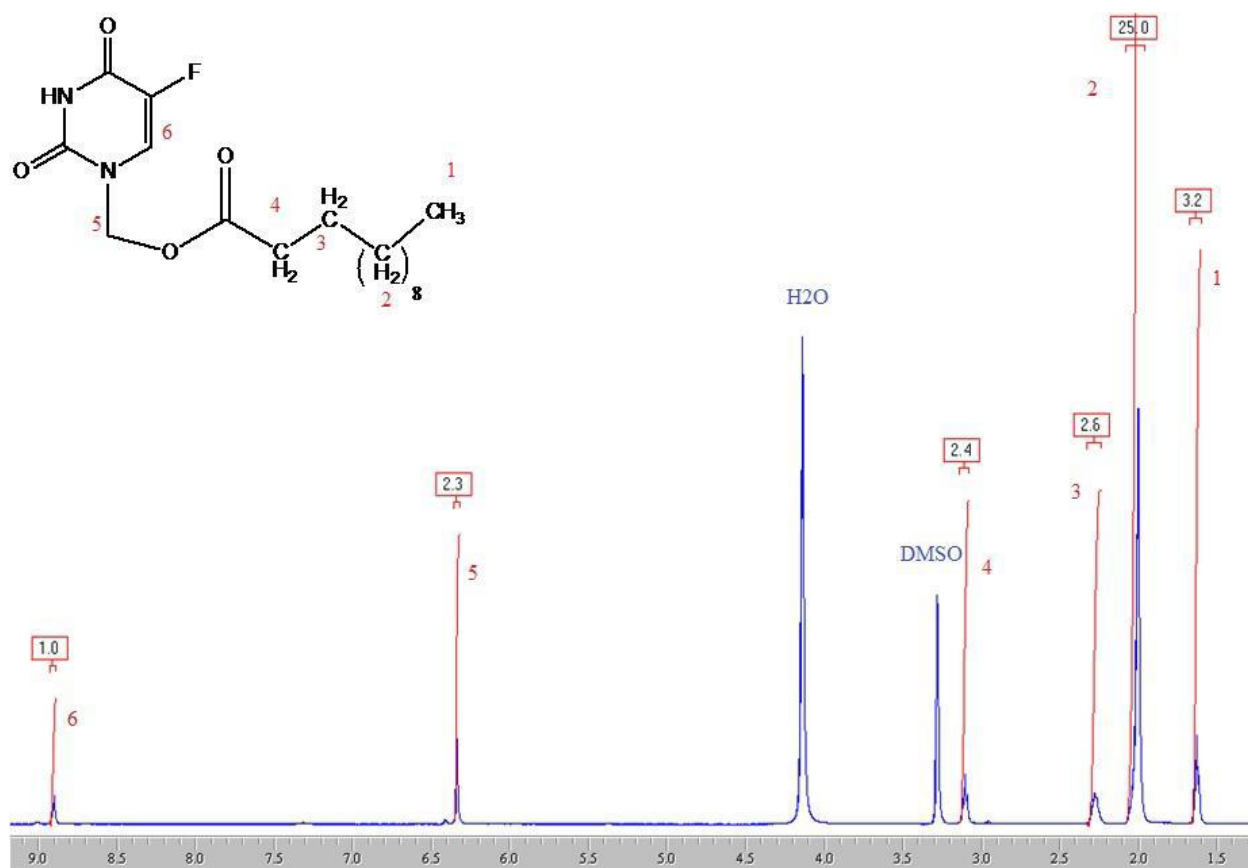
325

326 2.1.2 Characterization of 5-FU-C12: ¹H NMR

327 5-FU-C12 was characterized by ¹H NMR analysis and the spectrum obtained is reported in Figure 2. 5-
328 FU-C12 ¹H NMR spectrum clearly indicated that the peak at $\delta = 8.9$ ppm was due to the aromatic -CH
329 proton of 5-FU; peak at $\delta = 6.3$ ppm was due to -CH₂- of the bridging methylenic group between 5-FU
330 and lauric acid. Further, peaks at $\delta = 3.1, 2.3, 2.1$ and 1.7 ppm may be assigned to the methylenic groups
331 and terminal methyl group of the lauric acid chain.

332

333



334

335

335 **Figure 2** - ¹H NMR spectrum of 5-FU-C12.

336

337 2.1.3 Pre-formulation: Water solubility of 5-FU-C12

338 Water solubility of 5-FU-C12 was tested at two different temperature conditions (room temperature and
339 60 °C) as showed in table 1. The 5-FU derivative was practically insoluble in water as reported in table

340 1. This finding confirmed the increased hydrophobic behavior of 5-FU-C12 compared to 5-FU, which
 341 is normally soluble in water (12 g/L, data from "European Pharmacopoeia", 8Ed, 2014).

342
 343 **Table 1.** Solubility in water of 5-FU-C12 at different conditions (room temperature and 60°C).
 344

Condition	Initial conc. 5-FU-C12 (mg/mL)	5-FU-C12 dissolved (%)	Solubility (mg/mL)	
Room Temperature	1.38	1.02	0.01	Practically insoluble
60 °C	1.50	5.62	0.09	

345
 346 Subsequently, with the purpose of identify the most adequate solubilizing agent for 5-FU-C12 to
 347 formulate 5-FU-C12-loaded LNC, we tested the solubility in different oils and organic solvents (ethanol
 348 and acetone) (see Table 2). In particular, we evaluated a series of excipients that are generally used for
 349 the formulation of LNC [22, 25]. The solubility of 5-FU-C12 was also tested in the mixture of oil and
 350 surfactant (Labrafac® and Span® 80), currently used in other formulations to obtain loaded LNC [15].
 351 Solubilization of 5-FU-C12 in oils was not possible after simple vortex passage (the unbundling of the
 352 bottom required a lot of time and was not effective). Samples were then maintained under magnetic
 353 stirring for 24 h, and plunged in a water bath set at 60 °C. After 48 h, samples were centrifuged and
 354 macroscopic observation did not reveal presence of sediment. Assays to assess the amount of solubilized
 355 product were performed using HPLC according to the method described in the experimental section.
 356 The results are shown in Table 2.

357
 358 **Table 2.** Solubility of 5-FU-C12 in different oils (a) and class 3 solvents (b).

Class 3 solvent	Solubilizing agent	5-FU-C12 Solubility(mg/mL)
	Oils and surfactant	Acetone
Ethanol		3.81
Labrafac®		14.21
Captex® 8000		10.34
Span® 80		13.60
Mixture (Labrafac + Span 80)		15.05

359
 360 As further proof of the increased lipophilic behavior of the derivative, we calculated the cLogP value :
 361 it was 4.48 for 5-FU-C12, while the value for 5FU was -0.78.

362 363 2.2 Development and characterization of blank and 5-FU-loaded LNC

364 2.2.1 Physico-chemical characterization of blank and 5-FU-C12-loaded LNC

365 Blank and loaded LNC were obtained following the Phase Inversion Technique (PIT) previously
 366 described [15]. To load 5-FU-C12 into LNC, Labrafac® and Span® 80 were chosen for the first step of
 367 preparation (preliminary dissolution of the derivative before adding other components). The solubility
 368 of the active in the mixture of selected excipients (50/50 w/w) was confirmed using HPLC.

369 The results of the physicochemical characterization of blank and 5-FU-C12-loaded LNC obtained with
 370 this process are showed on Table 3. The average size for all the systems developed was approximately
 371 65 nm. The polydispersity index was below 0.1, indicating unimodal and narrow size distribution. The
 372 zeta potential values were neutral or slightly negative, ranging from -4 to -7 mV and corresponded to
 373 classical values obtained for LNC.

374 To evaluate the encapsulation efficiency of the drug into the LNC, samples of 5-FU-C12-loaded LNC
 375 were prepared and purified through 0.22 μm filtration prior to HPLC analysis. As indicated, the
 376 encapsulation efficiency at different payloads was high, around 98%. This result was due to the high
 377 hydrophobicity of the derivative, which was dissolved in the oily hydrophobic core of LNC. Finally, the
 378 endotoxin content was assessed and the value was under 5 EU/mL for every batch (data not shown)
 379 according to the Ph Eur 9 and under GMP conditions. The value obtained for the endotoxin content was
 380 consistent with an IV administration of the LNC.

381

382 **Table 3.** Physicochemical characterization of blank and 5-FU-C12-loaded LNC.

383

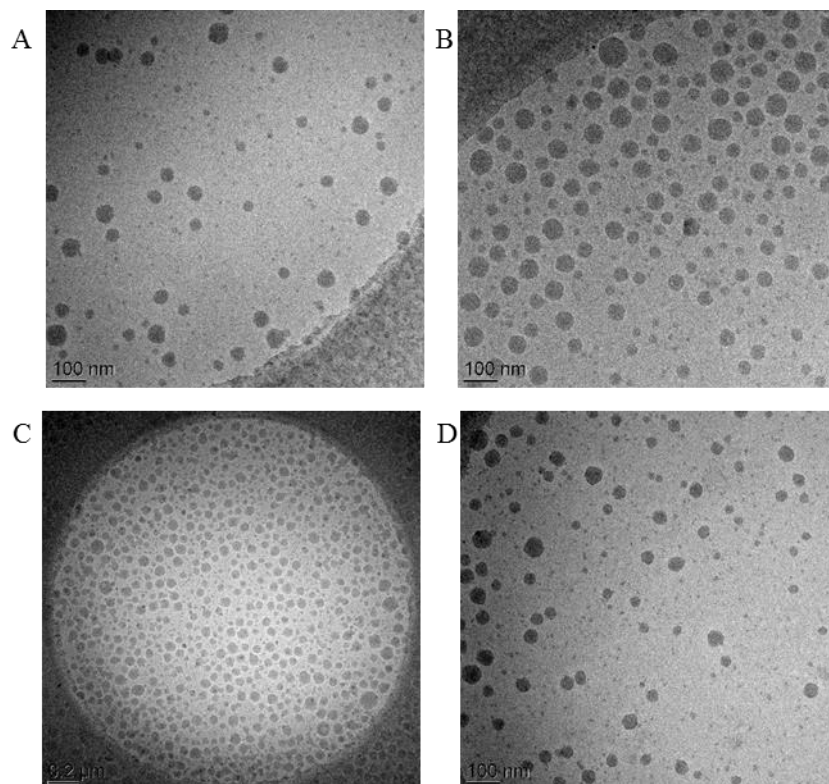
Formulation	Size* (nm)	PDI	ζ -potential* (mV)	5-FU-C12 payload* (mg/g)
Blank LNC	65 \pm 3	<0.1	-6 \pm 1	-
5-FU-C12-loaded LNC	65 \pm 2	<0.1	-4 \pm 2	1.7 \pm 0.1
	64 \pm 3	<0.1	-2 \pm 1	2.4 \pm 0.2
	64 \pm 1	<0.1	-4 \pm 2	4.5 \pm 0.1

384 *Data represent average \pm S.D.; PDI: polydispersion index, 5-FU-derivative payload = mg of 5-FU-
 385 derivative/g of LNC dispersion

386

387 A cryoTEM analysis of blank and 5-FU-C12-loaded LNC diluted twice in water, are shown in Figure
 388 3. A cryoTEM observation was chosen in addition to the DLS technique because it allowed to
 389 discriminate the contribution of small versus big particles as DLS presented the size as a mean
 390 hydrodynamic radius and could therefore be biased by extreme sizes of nanoparticles [26]. Both LNC
 391 formulations presented almost no dispersed population with spherical shape and no differences were
 392 found between empty and loaded systems.

393



394

395 **Figure 3:** Microstructure obtained by cryoTEM of blank (A and B) and LNC loaded with 1.7 mg/g of
396 5-FU-C12 (C and D).

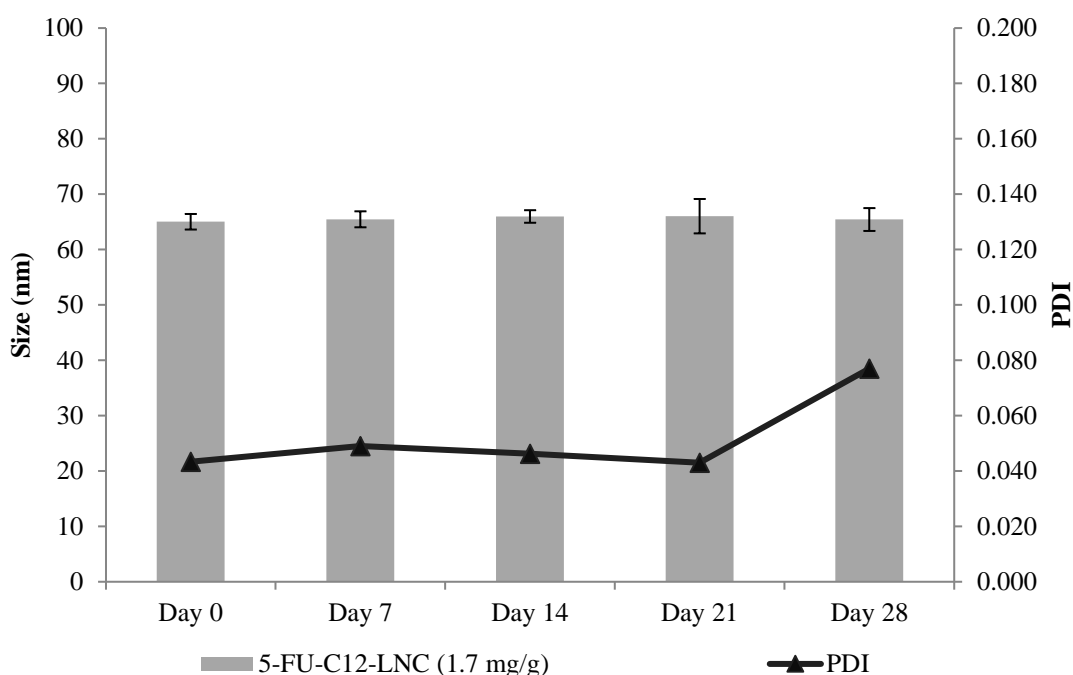
397

398

399 2.2.3 Storage stability in aqueous suspension

400 The different batches of 5-FU-C12-loaded LNC were stable over one month, indeed, no differences
401 were observed in the average size, while a small increase in the PDI value, which remains below the
402 value of 0.1, was observed after 1 month as shown in Figure 4.

403 In addition, stability studies of the drug-loaded nanosystems were performed to evaluate the leakage of
404 the derivative from the LNC at different payloads after 1 month of storage in water suspension
405 (measurement of variation in the drug payload and, consequently, in the rate of encapsulation). No
406 leakage of the derivative from the nanocapsules was detected over the period studied.

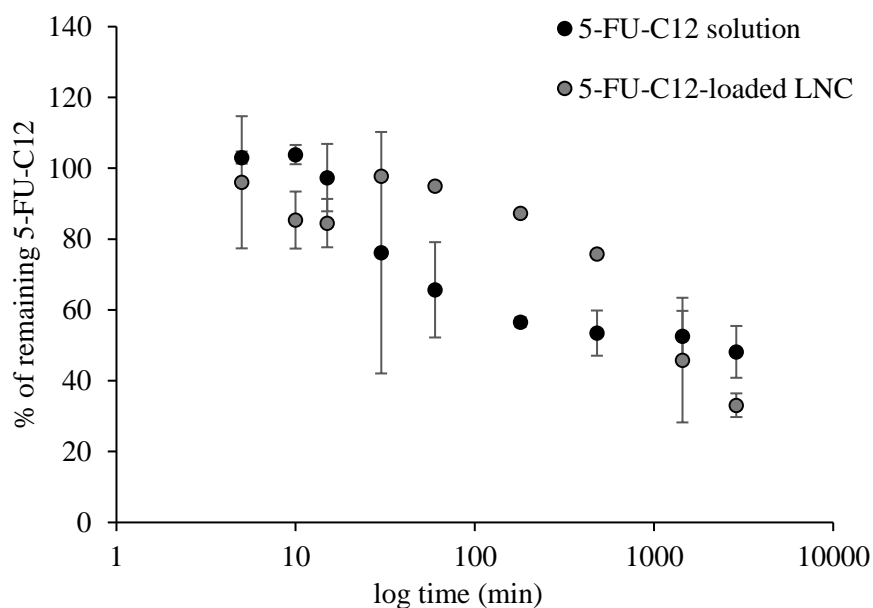


407
408 **Figure 4.** Size and PDI evolution over time of 5-FU-C12-loaded (1.7 mg/g) LNC in suspension at 4°C
409 (n=3).
410

411 An *in vitro* release study to check the release of the drug from the nanocarriers, for the formulation with
412 5-FU-C12-loaded in the LNC, was carried out in PBS/Tween® 80. This experiment showed that 5-FU-
413 C12 was not released from the LNC over 24h of incubation. Indeed, thanks to the hydrophobicity of the
414 derivative, the drug was completely retained into the nanosystem.

415 2.2.3 Stability in plasma

416
417 Subsequently, the stability of encapsulated 5-FU derivative in LNC was also investigated in human
418 plasma by measuring with HPLC method the percentage of remaining intact drug over time. 5-FU-C12
419 acetone solution in was also tested. As shown in Figure 5, the drug integrity was maintained in its free
420 form during the first 15 min, then the concentration decreased and only 50% of the drug was detected
421 after 1h of incubation. In the case of encapsulated 5-FU-C12, almost 100 % of the drug was detected
422 following 3h of incubation and 50% of the initial content was stable until 24 h of incubation. The
423 improvement in drug stability detected at least during the first 3h of incubation is ascribed to LNC
424 encapsulation and hence protection from rapid elimination.



425 **Figure 5:** Stability of 5-FU-C12 following incubation of drug solution or encapsulated in LNC in human
 426 plasma. Time (min) is represented in log scale.
 427
 428

429
 430 **2.3 Scale up of blank and 5FU-C12 loadedLNC**
 431

432 In order to scale up the LNC formulation using the phase inversion method, two large volume batches
 433 were prepared in order to evaluate the robustness of the formulation process. Firstly, an intermediate
 434 batch corresponding to a batch ten times bigger than the laboratory one was produced. Then, a second
 435 batch twenty-fold bigger was obtained. The physico-chemical characteristics of both batches in terms
 436 of size, polydispersity index and zeta potential were assessed and the results of the characterization are
 437 reported in table 4. No significant differences were found comparing the laboratory batch (scale x1) and
 438 the scale up batches (scale x10 corresponding to 56g of formulation and scale x20 corresponding to
 439 112g of formulation). The LNC maintained their initial properties in terms of size and polydispersion
 440 indicating that the process was transposable to industrial settings.

441
 442 **Table 4:** Physico-chemical characterization of blank LNC at different batch scales
 443

Time	Scale x1 = 5.6g			Scale x10 = 56g			Scale x20 = 112g		
	Size (nm)	PDI	ζ-potential (mV)	Size (nm)	PDI	ζ-potential (mV)	Size (nm)	PDI	ζ-potential (mV)
1 month	65±2	<0.1	-	70±2	<0.1		70±2	<0.1	-10.2±2
2 months	73±3	<0.1	-6.68±2	66±2	<0.1	-5.84	73±2	<0.1	nd

446 2.4 *In vitro* cell studies

447 2.4.1 *In vitro* cytotoxicity on 2D cell growth

448 In order to analyze the biological effect of the preparations, we tested the viability of glioma (9L) and
449 colon cancer (HCT-116) cells following 48h of treatment with escalating doses of different formulations
450 by using the MTS assay. We also tested the incubation of the systems during 24h, however the reduction
451 in cell viability was not important and we decided to increase exposure time.

452 5-FU derivative in the free form (5-FU-C12 solubilized in acetone) or encapsulated into LNC compared
453 to native 5-FU aqueous solution were tested. Blank LNC were also tested as control to exclude toxic
454 effects of the nanocarriers. The results expressed in percentage of viability at different concentrations
455 are reported in Figure 6.

456

457

458

459

460

461

462

463

464

465

466

467

468

469

470

471

472

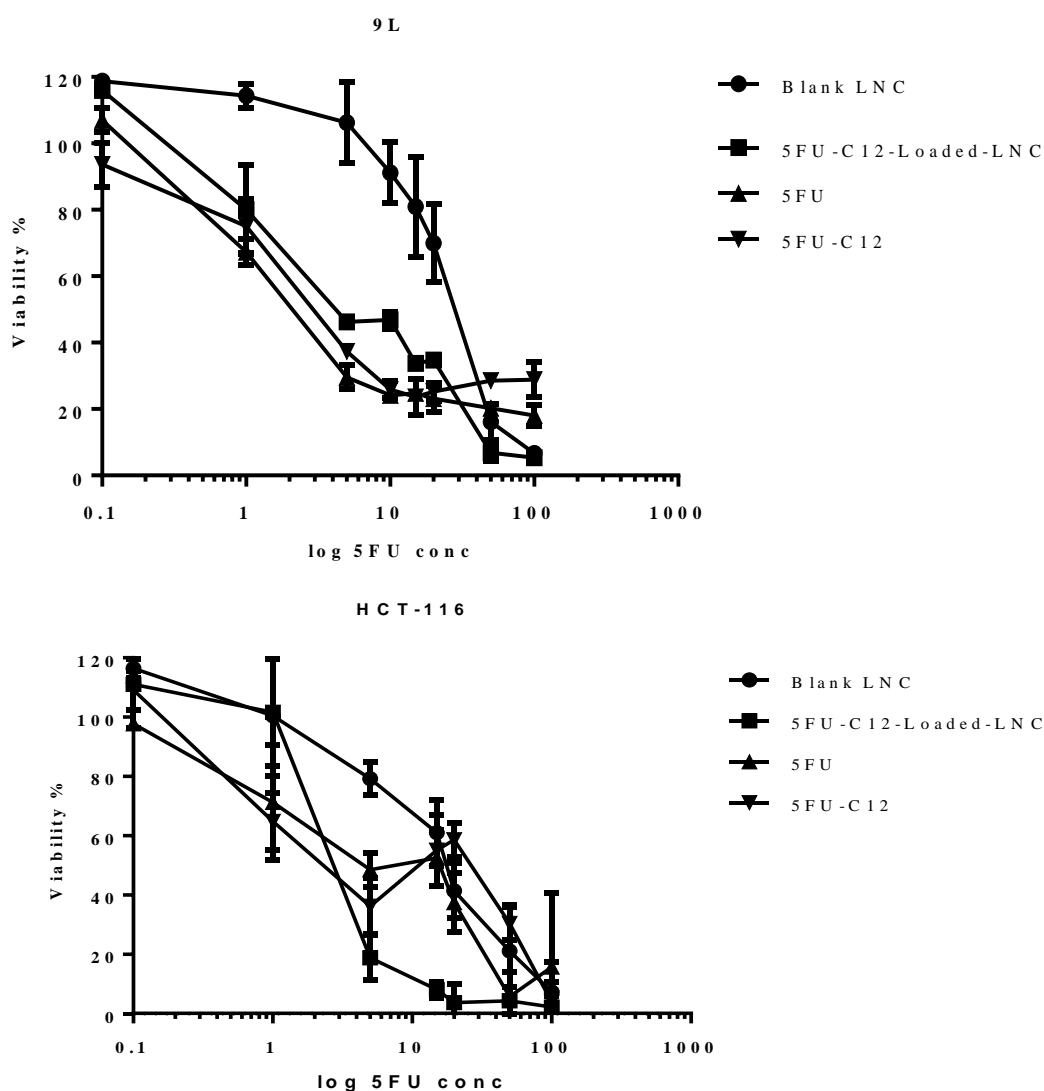
473

474

475

476

477



477

478 **Figure 6.** Cell viability of 9L and HCT-116 cells vs drug concentration after 48h incubation (37 °C)
479 with blank and 5-FU-C12-loaded LNC, compared to free 5-FU (solution in water) and 5-FU-C12
480 (solution in acetone). Drug concentration is presented in log scale (n=5; mean ± S.D.).

481 After 48h of exposure to 5-FU-C12-loaded LNC, viability decreased as a function of the drug
 482 concentration exposure for both cell lines tested (Figure 6). IC50 values for drug (concentration μM)
 483 and LNC treatments (concentration mg/mL) and the respective confidence interval (μM or mg/ml), are
 484 shown in Table 5.

485
 486 **Table 5.** IC50 (μM) and (mg/mL of LNC) of 5-FU-C12-loaded LNC compared to 5-FU-C12 derivative,
 487 5-FU aqueous solution and blank LNC on 9L and HCT-116 cell line.

Formulation	IC50 (5FU μM) and CI		IC50 (mg/mL LNC) and CI	
	9L	HCT-116	9L	HCT-116
Blank LNC	-	-	0.77 (0.53, 0.97)	0.193 (0.082, 0.457)
5-FU-C12 LNC	2.24 (1.75, 2.86)	2.48 (1.45, 4.22)	0.22 (0.17, 0.29)	0.058 (0.033, 0.098)
5-FU-C12 solution	16.91 (15.50, 22.88)	20.72 (11.20, 38.35)	-	-
5-FU water solution	9.09 (3.48, 23.78)	4.08 (1.056, 21.86)	-	-

488
 489 A moderate cytotoxic effect on 9L cell line of 5-FU compared to 5-FU-C12 solution was found, the
 490 IC50 values being 9.09 and 16.91 μM , respectively. However, when the 5-FU-C12 was encapsulated
 491 into LNC, the cytotoxic effect was more pronounced with an IC50 value of 2.24 μM . Cytotoxicity on
 492 9L cell line was observed for blank LNC (non-loaded nanocarrier dispersions diluted in culture medium
 493 at the same excipients concentration than that needed for loaded ones) only at high concentration around
 494 0.77 mg/mL.

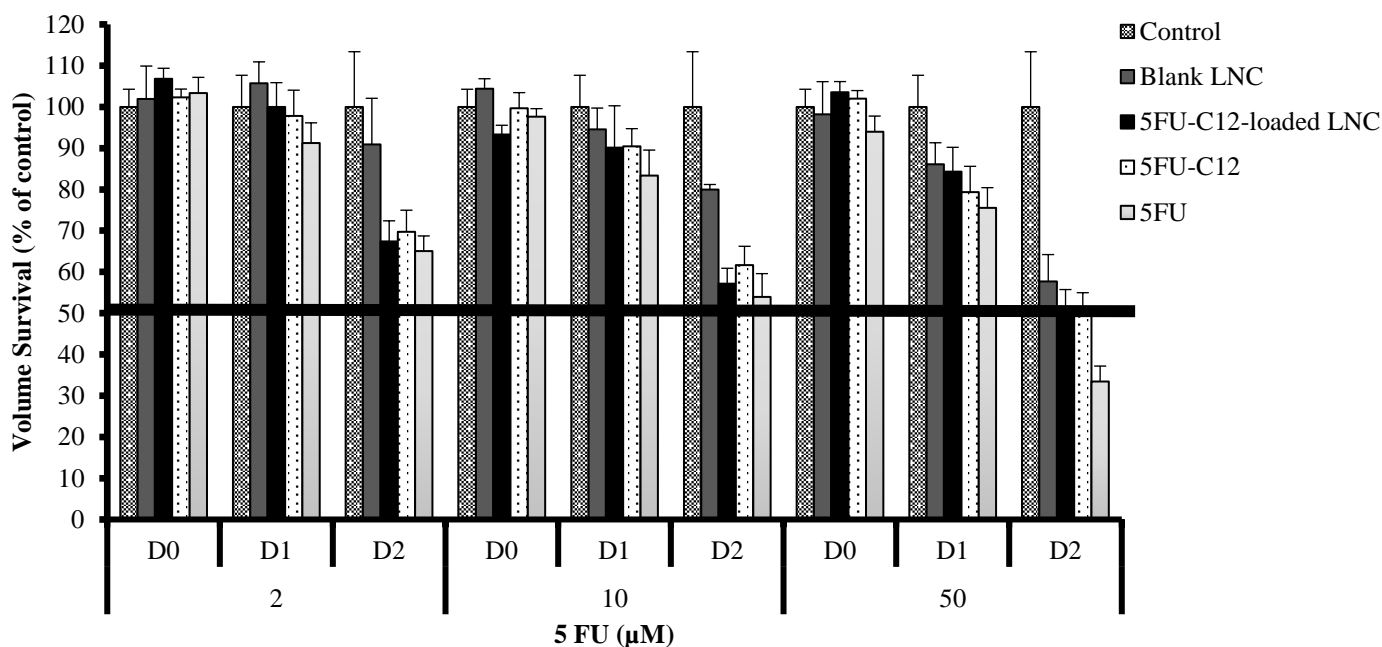
495 The viability of HCT-116 cells exposed to different concentrations of 5-FU alone or encapsulated into
 496 LNC was determined following 48 h of treatment. Pure 5-FU (water solution) was more effective than
 497 5-FU-C12 solution being the values of IC50 of 4.8 and 20.72 μM respectively. 5-FU-C12-loaded LNC
 498 showed a toxic effect more pronounced as compared with free drug being the IC50 value of 2.48 μM .
 499 Blank LNC were 3 times less toxic as compared to the loaded system being the values 0.193 and 0.053
 500 mg/ml respectively (Table 5).

501 502 2.4.2 *In vitro* cytotoxicity on 3D cell growth

503 To establish the impact on tumor viability of our formulations on a more lifelike *in vitro* culture system,
 504 we tested the dose response of 5-FU solution in comparison with the modified 5-FU-C12-loaded LNC
 505 during a 48 h treatment on a MultiCellular Tumor Spheroids (MCTS) derived from the HCT-116 cell
 506 line (Methods). The volume of MCTS was evaluated from phase contrast microscopy images (Methods)
 507 as a readout of cytotoxic effect. The data reported in Figure 7 represent normalized MCTS volume for
 508 different drug treatments with respect to the control volume (MCTS not treated). Three different drug
 509 concentrations were tested: 2, 10 and 50 μM of 5-FU, 5-FU-C12 and 5-FU-C12 –loaded LNC.

510 As showed in the figure 7, loaded-LNC with modified 5-FU-C12 and 5-FU-C12 or 5-FU in solution
511 were able to reduce the volume of the spheroids after 2 days of treatment (D2) even at drug doses of 2
512 μM . The cytotoxic effect was more pronounced at higher doses (10 and 50 μM).

513 Similar to the non-specific toxicity observed in 2D cell culture, blank LNC induced a slight reduction
514 of MCTS volume only at very high drug concentration.



515

516

517 **Figure 7:** Normalized volume of multicellular HT116 spheroids after treatment with blank LNC, LNC
518 loaded with 5-FU-C12, modified 5-FU-C12 dissolved in acetone and 5-FU clinical formulation.
519 Spheroids were treated with different drug concentrations (2, 10 and 50 μM) at different time points
520 (Day 0, Day 1 and Day 2).

521

522 3 Discussion

523 5-FU is common chemotherapeutic agent used for the treatment of different cancers [27]. Its rapid
524 catabolism, short half-life (15-20 min), indiscriminate biodistribution, aspecific cytotoxicity and
525 myelosuppression impose the need to develop an alternative formulation and delivery system for this
526 anticancer drug [27]. When administered intravenously, approximately 90% of an injected dose of 5-
527 FU is metabolized to inactive 5-FUH₂ by DPD in the liver, peripheral blood mononuclear cells,
528 intestinal mucosa, pancreas, lungs and kidneys, thus limiting its efficacy. Thus, the maintenance of a
529 therapeutic serum concentration requires continuous administration of high doses of this drug with
530 subsequent severe toxic effects [6]. To solve the limitations related with 5-FU administration, two main
531 strategies have been investigated in the present work: i) the synthesis of novel 5-FU derivative and ii)
532 the encapsulation of this active into lipid nanocapsules. As compared to other lipid-based nanocarriers
533 like liposomes, LNC display some convenient features; in fact, they are prepared by an organic solvent
534 free and soft-energy procedure and present great storage stability [15]. In addition, physicochemical
535 properties of optimal LNC (i.e. size range, polydispersity index) can be monitored and designed ad hoc,

536 since they are strongly dependent on the proportions of different components (oily phase, hydrophilic
537 surfactant, aqueous phase - water plus sodium chloride).

538 Different studies report attempts to improve the *in vivo* performances of 5FU, through the development
539 of prodrugs and encapsulation in drug delivery nanosystems [8, 16, 28]. However, the inherent
540 hydrophilic nature of 5-FU, and low encapsulation efficiency was observed for different nanocarriers
541 [16]. In our work, 5-FU was modified with a biocompatible moiety, lauric acid, to obtain a lipid–drug
542 conjugate having more affinity for the hydrophobic core of the LNC (production yield of 70%). The
543 easy synthesis and higher degree of purification ensured the complete elimination of formaldehyde in
544 the first step of the synthesis (Figure 1). 5-FU-C12 was characterized by nuclear magnetic resonance
545 (NMR) and the ¹H NMR (Figure 2) indicates that only one chain of lauric acid was conjugated to the
546 N1 position. Previously, a derivative of 5-FU named 5-FUDIPAL obtained by conjugating palmitic acid
547 to the drug was published. In this compound, two lipid tails were attached to the lipid–5-FU conjugate
548 (in N1 and N3 position) which imparted hydrophobic characteristics to 5-FU [23]. In our case, the
549 conjugation of only a single chain of lauric acid to N1 position strongly affects the hydrophobicity of
550 the novel compound, 5-FU-C12. Indeed, pre-formulation solubility studies carried out in a polar solvent
551 (water), non-polar solvents (acetone and ethanol), oils and surfactants demonstrated that 5-FU-C12 was
552 not soluble in water while freely soluble in polar solvents and oils. Its hydrophobicity makes 5-FU-C12
553 a suitable candidate for LNC encapsulation. In Figure 3, we demonstrated that LNC loaded with 5-FU
554 derivative with a hydrodynamic size of around 65 nm and a neutral surface charge. Using the PIT
555 method, spherical and monodispersed systems, also confirmed by cryoTEM images, were obtained
556 (Figure 3). The conjugated lauric acid tail was expected to elevate the non-covalent interaction between
557 the drug and the oily core of the system resulting in a high amount of drug loading and absence of fast
558 release. Moreover, the encapsulation provides protection to the drug from plasmatic degradation. 5-FU-
559 C12-loaded LNC were incubated with human plasma and the drug was detected until 3h following
560 incubation, while 5-FU-C12 was eliminated earlier being detected only 1h following incubation (Figure
561 5). Considering that the plasmatic half-life of 5FU is of around 30 min [29], the LNC here developed
562 led to an important increase in drug detection when incubated with plasma.

563 The biological evaluation of 5-FU-C12 on 2D cell culture measured by MTS showed that 5-FU-C12-
564 loaded LNC had an enhanced cytotoxic effect on 9L and HTC-116 cell line in comparison with modified
565 drug alone, being the IC₅₀ values eight and ten times lower compared to the 5-FU-12 alone. Also,
566 loaded-LNC were more cytotoxic with respect to 5FU. It was reported that following 48h of treatment
567 on HCT-116 cells, the IC₅₀ value of PLGA nanoparticles loaded with 5-FUDIPAL, a similar palmitic-
568 acid conjugate, was around 23 μM [23], twenty times higher in comparison to the IC₅₀ value of 5-FU-
569 C12-loaded LNC (IC₅₀ around 2 μM). Besides, 5-FU-loaded pH-sensitive liposomes having different
570 lipid compositions had been also described and their activity tested on HCT-116 cell line. The authors
571 found differences in cell sensitivity when treated with the formulation obtained and ascribed the
572 differences and the resulting low anti-cancer activity of liposomes to the low entrapment efficiency of

573 5-FU [30]. Low encapsulation efficiency and premature release of the drug strongly affect the efficacy
574 of the nanosystems encapsulating 5-FU in these nanosystems. Comparing the results on HCT-116 cell
575 line to other nanosystems loaded with 5-FU derivative, the encapsulation into LNC was more effective
576 in reducing cell viability. 5-FU-C12 loaded LNC here developed were able to encapsulate in a high
577 amount the novel hydrophobic compound and to retain the drug in the oil core even when diluted in
578 simulated physiological media, therefore promising to increase the half-life of the drug.

579 In a 2D cell model free drug or nanosystems had to enter into a cell monolayer to exert their cytotoxic
580 activity. The difference in the cytotoxic effect is related to the stability, solubility, release and
581 internalization ability of drug when enter cells. From our result is evident that the encapsulation of the
582 5-FU-C12 enhanced the stability and internalization of the drug, being the effect of drug loaded LNC
583 more pronounced in comparison to free drug.

584 Once we demonstrated the enhanced cytotoxic effect of drug loaded-LNC on 2D cell culture, HCT-116
585 cells were used to form 3D spheroids and the effect of the 2 days of treatment, with 5-FU-C12 loaded
586 LNC, 5-FU or 5-FU-C12 alone was investigated. The aim was to test the LNC developed in a more
587 complex system that mimics the 3D chemical and physical gradients that occur in *in vivo* tumors. The
588 volume of the spheroids was measured as a readout for cytotoxicity after 24 and 48h of treatment. As
589 showed in Figure 7, for all the treatments we observed a reduction of MCTS volume as time increases,
590 demonstrating the inhibition of MCTS growth. Interestingly, the effect of drugs alone and 5-FU-C12
591 loaded LNC had a similar effect on MCTS volume, suggesting a comparable efficacy in 3D systems.
592 Moreover, the effect of blank LNC on MCTS growth is less pronounced than that of loaded LNC. This
593 observation is particularly evident at day 2 at the highest concentration tested (0.875 mg/ml). This result
594 contrasts with the observations made on the 2D cell model, where the non-specific toxicity of blank
595 LNC appears at lower concentration (0.193 mg/ml). This difference should be analyzed considering that
596 we used different readouts for the efficacy in 2D and 3D cell model [31]. In 2D we evaluated cell death
597 through a metabolic assay (MTS) while in 3D we evaluated MCTS growth, which results from the
598 equilibrium between cell death and proliferation. The difference we observe thus suggests that blank
599 LNC causes cell death, which is the origin of their toxicity, but does not affect cell proliferation. In
600 future works, there are many parameters that should investigated to confirm this analysis, such as
601 permeability of the spheroids to the treatment [32, 33].

602 Globally, from the preliminary results, we observed that the encapsulation into LNC does not hamper
603 the penetration into the spheroid, and enhance cytotoxic effect respect to the other treatments. Further
604 in depth studies taking into account permeability, distribution of the drug and mechanism of
605 internalization of drug loaded LNC into MCTS has to be performed to fully disclose the efficacy of this
606 system.

607

608 **Conclusion**

609 In the present work, we reported evidence about the feasibility of an oily-core nanoformulation for 5-
610 FU-derivative encapsulation. Using a simple synthesis process, we develop with a high yield of
611 production a novel lipophilic 5FU derivative namely 5-FU-C12, which was successfully encapsulated
612 into LNC. The novel formulation obtained enhanced the solubility and the stability of the drug when in
613 contact with plasma. Further, *in vitro* studies were carried out in different tumor cell lines (9L and HCT-
614 116) to assess the cytotoxic activity of the encapsulated drug in respect to the drug in solution or the
615 commercial one. 5-FU-C12-loaded LNC resulted in a higher cytotoxic effect compared with 5-FU-C12
616 alone or 5FU while blank LNC showed cytotoxic ability only at very high concentrations indicating
617 possible limited toxic effects of the carriers. Then, to obtain reliable and detailed information about
618 LNC-tumor interaction in a more physiologic situation we analyzed the effects of the treatments on
619 HCT-116 3D-spheroid-cultures. The results evidenced that the effect on spheroids survival was at least
620 similar between drug-loaded LNC, 5-FU-C12 and 5-FU alone. We can therefore state that the fact that
621 it has encapsulated in a complex system does not reduce the penetration capacity of the spheroids.
622 Further research will be needed to make these nanosystems not only comparable to solution treatments
623 in their effect on 3D systems but to make them more effective.

624

625 **Acknowledgments**

626 Authors are thankful to Pierre-Yves Dugas from the Univ Lyon, Université Claude Bernard Lyon 1,
627 CNRS, C2P2 UMR 5265, for his kind help and expertise for cryoTEM observation, and to Thomas
628 Perrier from Carlina Techology, for his kind help with the stability studies in plasma.

629 This work has been carried out within the research program of NICHE, financially supported by
630 EuroNanoMed-II (4th call) and RESOLVE, financially supported by EuroNanoMed-III (8th call).

631

632 **Bibliography**

633

- 634 1. Longley DB, Harkin DP, Johnston PG. 5-Fluorouracil: mechanisms of action and
635 clinical strategies [Review Article]. *Nature Reviews Cancer*. 2003;3:330. doi:
636 10.1038/nrc1074.
- 637 2. Vincent J, Mignot G, Chalmin F, et al. 5-Fluorouracil Selectively Kills Tumor-
638 Associated Myeloid-Derived Suppressor Cells Resulting in Enhanced T Cell-
639 Dependent Antitumor Immunity. *Cancer Research*. 2010;70(8):3052-3061. doi:
640 10.1158/0008-5472.can-09-3690.
- 641 3. Ugel S, Delpozzi F, Desantis G, et al. Therapeutic targeting of myeloid-derived
642 suppressor cells. *Current Opinion in Pharmacology*. 2009 2009/08/01/;9(4):470-481.
643 doi: <https://doi.org/10.1016/j.coph.2009.06.014>.
- 644 4. Neto OV, Raymundo S, Franzoi MA, et al. DPD functional tests in plasma, fresh saliva
645 and dried saliva samples as predictors of 5-fluorouracil exposure and occurrence of
646 drug-related severe toxicity. *Clinical Biochemistry*. 2018 2018/04/04/. doi:
647 <https://doi.org/10.1016/j.clinbiochem.2018.04.001>.
- 648 5. Yang CG, Ciccolini J, Blesius A, et al. DPD-based adaptive dosing of 5-FU in patients
649 with head and neck cancer: impact on treatment efficacy and toxicity. *Cancer*

- 650 Chemotherapy and Pharmacology. 2011 2011/01/01;67(1):49-56. doi: 10.1007/s00280-
651 010-1282-4.
- 652 6. Lee JJ, Beumer JH, Chu E. Therapeutic drug monitoring of 5-fluorouracil. Cancer
653 Chemotherapy and Pharmacology. 2016 2016/09/01;78(3):447-464. doi:
654 10.1007/s00280-016-3054-2.
- 655 7. S E Ward EK, J Cowan, M Marples, B Orr, and M T Seymour. The clinical and economic
656 benefits of capecitabine and tegafur with uracil in metastatic colorectal cancer. Br J
657 Cancer. 2006;3(95):1.
- 658 8. Álvarez P, Marchal JA, Boulaiz H, et al. 5-Fluorouracil derivatives: a patent review.
659 Expert Opinion on Therapeutic Patents. 2012 2012/02/01;22(2):107-123. doi:
660 10.1517/13543776.2012.661413.
- 661 9. P Cellier BL, L Martin, B Vié, C Chevelle, V Vendrely, A Salemkour, C Carrie, G
662 Calais, P Burtin, L Champion, M Boisdron-Celle, A Morel, V Berger, E Gamelin. Phase
663 II study of preoperative radiation plus concurrent daily tegafur-uracil (UFT) with
664 leucovorin for locally advanced rectal cancer. BMC Cancer. 2011;11:98.
- 665 10. Zhang M WW, Liu J, Yang H, Jiang Y, Tang W, Li Q, Liao X. Comparison of the
666 effectiveness and toxicity of neoadjuvant chemotherapy regimens,
667 capecitabine/epirubicin/cyclophosphamide vs 5-
668 fluorouracil/epirubicin/cyclophosphamide, followed by adjuvant,
669 capecitabine/docetaxel vs docetaxel, in patients with operable breast cancer. Onco
670 Targets Ther. 2016 8(9):3443-50.
- 671 11. Henderson LA, Shankar LK. Clinical Translation of the National Institutes of Health's
672 Investments in Nanodrug Products and Devices. The AAPS Journal. 2017
673 2017/03/01;19(2):343-359. doi: 10.1208/s12248-016-9995-x.
- 674 12. Grabbe S, Haas H, Diken M, et al. Translating nanoparticulate-personalized cancer
675 vaccines into clinical applications: case study with RNA-lipoplexes for the treatment of
676 melanoma. Nanomedicine. 2016;11(20):2723-2734. doi: 10.2217/nmm-2016-0275.
677 PubMed PMID: 27700619.
- 678 13. Sykes EA, Dai Q, Sarsons CD, et al. Tailoring nanoparticle designs to target cancer
679 based on tumor pathophysiology. Proceedings of the National Academy of Sciences.
680 2016;113(9):E1142-E1151. doi: 10.1073/pnas.1521265113.
- 681 14. Lollo G, Hervella P, Calvo P, et al. Enhanced in vivo therapeutic efficacy of plitidepsin-
682 loaded nanocapsules decorated with a new poly-aminoacid-PEG derivative.
683 International Journal of Pharmaceutics. 2015 2015/04/10;483(1):212-219. doi:
684 <https://doi.org/10.1016/j.ijpharm.2015.02.028>.
- 685 15. Sasso MS, Lollo G, Pitorre M, et al. Low dose gemcitabine-loaded lipid nanocapsules
686 target monocytic myeloid-derived suppressor cells and potentiate cancer
687 immunotherapy. Biomaterials. 2016 2016/07/01;96:47-62. doi:
688 <https://doi.org/10.1016/j.biomaterials.2016.04.010>.
- 689 16. Fanciullino R, Mollard S, Giacometti S, et al. In Vitro and In Vivo Evaluation of
690 Lipofufol, a New Triple Stealth Liposomal Formulation of Modulated 5-Fu: Impact on
691 Efficacy and Toxicity. Pharmaceutical Research. 2013 2013/05/01;30(5):1281-1290.
692 doi: 10.1007/s11095-012-0967-2.
- 693 17. Roullin V-G, Deverre J-R, Lemaire L, et al. Anti-cancer drug diffusion within living rat
694 brain tissue: an experimental study using [3H](6)-5-fluorouracil-loaded PLGA
695 microspheres. European Journal of Pharmaceutics and Biopharmaceutics. 2002
696 2002/05/01;53(3):293-299. doi: [https://doi.org/10.1016/S0939-6411\(02\)00011-5](https://doi.org/10.1016/S0939-6411(02)00011-5).
- 697 18. Patel MN, Lakkadwala S, Majrad MS, et al. Characterization and Evaluation of 5-
698 Fluorouracil-Loaded Solid Lipid Nanoparticles Prepared via a Temperature-Modulated

- 699 Solidification Technique. *AAPS PharmSciTech*. 2014 2014/12/01;15(6):1498-1508.
700 doi: 10.1208/s12249-014-0168-x.
- 701 19. Liu Z, Fullwood N, Rimmer S. Synthesis of allyloxycarbonyloxymethyl-5-fluorouracil
702 and copolymerizations with -vinylpyrrolidinone [10.1039/B002092N]. *Journal of*
703 *Materials Chemistry*. 2000;10(8):1771-1775. doi: 10.1039/b002092n.
- 704 20. Liu Z, Rimmer S. Synthesis and release of 5-fluorouracil from poly(N-
705 vinylpyrrolidinone) bearing 5-fluorouracil derivatives. *Journal of Controlled Release*.
706 2002 2002/05/17;81(1):91-99. doi: [https://doi.org/10.1016/S0168-3659\(02\)00048-2](https://doi.org/10.1016/S0168-3659(02)00048-2).
- 707 21. B. Heurtault PS, B. Pech, J. E. Proust, and J. P. Benoit. A novel phase inversion -based
708 process for the preparation of lipid nanocarrier. *Pharm Res*. 2002;19(6):875–880.
- 709 22. Moysan E, Gonzalez-Fernandez Y, Lautram N, et al. An innovative hydrogel of
710 gemcitabine-loaded lipid nanocapsules: when the drug is a key player of the
711 nanomedicine structure [10.1039/C3SM52781F]. *Soft Matter*. 2014;10(11):1767-1777.
712 doi: 10.1039/c3sm52781f.
- 713 23. Ashwanikumar N, Kumar NA, Asha Nair S, et al. 5-Fluorouracil–lipid conjugate:
714 Potential candidate for drug delivery through encapsulation in hydrophobic polyester-
715 based nanoparticles. *Acta Biomaterialia*. 2014 2014/11/01;10(11):4685-4694. doi:
716 <https://doi.org/10.1016/j.actbio.2014.07.032>.
- 717 24. Virgone-Carlotta A, Lemasson M, Mertani HC, et al. In-depth phenotypic
718 characterization of multicellular tumor spheroids: Effects of 5-Fluorouracil. *PLOS*
719 *ONE*. 2017;12(11):e0188100. doi: 10.1371/journal.pone.0188100.
- 720 25. Lollo G, Vincent M, Ullio-Gamboa G, et al. Development of multifunctional lipid
721 nanocapsules for the co-delivery of paclitaxel and CpG-ODN in the treatment of
722 glioblastoma. *International Journal of Pharmaceutics*. 2015 2015/11/30;495(2):972-
723 980. doi: <https://doi.org/10.1016/j.ijpharm.2015.09.062>.
- 724 26. Wibroe PP, Ahmadvand D, Oghabian MA, et al. An integrated assessment of
725 morphology, size, and complement activation of the PEGylated liposomal doxorubicin
726 products Doxil®, Caelyx®, DOXOrubicin, and SinaDoxosome. *Journal of Controlled*
727 *Release*. 2016 2016/01/10;221:1-8. doi: <https://doi.org/10.1016/j.jconrel.2015.11.021>.
- 728 27. Gusella M, Crepaldi G, Barile C, et al. Pharmacokinetic and demographic markers of
729 5-fluorouracil toxicity in 181 patients on adjuvant therapy for colorectal cancer. *Annals*
730 *of Oncology*. 2006;17(11):1656-1660. doi: 10.1093/annonc/mdl284.
- 731 28. Carrillo E, Navarro SA, Ramírez A, et al. 5-Fluorouracil derivatives: a patent review
732 (2012 – 2014). *Expert Opinion on Therapeutic Patents*. 2015 2015/10/03;25(10):1131-
733 1144. doi: 10.1517/13543776.2015.1056736.
- 734 29. Bocci G, Danesi R, Di Paolo A, et al. Comparative Pharmacokinetic Analysis of 5-
735 Fluorouracil and Its Major Metabolite 5-Fluoro-5,6-dihydrouracil after Conventional
736 and Reduced Test Dose in Cancer Patients. *Clinical Cancer Research*. 2000;6(8):3032-
737 3037.
- 738 30. Udofot O AK, Israel B, Agyare E. Cytotoxicity of 5-fluorouracil-loaded pH-sensitive
739 liposomal nanoparticles in colorectal cancer cell lines. *Integr Cancer Sci Ther*.
740 2015;2(5):245-252.
- 741 31. Solomon MA, Lemera J, D’Souza GGM. Development of an in vitro tumor spheroid
742 culture model amenable to high-throughput testing of potential anticancer
743 nanotherapeutics. *Journal of Liposome Research*. 2016 2016/07/02;26(3):246-260. doi:
744 10.3109/08982104.2015.1105820.
- 745 32. Ho WY, Yeap SK, Ho CL, et al. Development of Multicellular Tumor Spheroid
746 (MCTS) Culture from Breast Cancer Cell and a High Throughput Screening Method
747 Using the MTT Assay. *PLOS ONE*. 2012;7(9):e44640. doi:
748 10.1371/journal.pone.0044640. PubMed PMID: PMC3435305.

749 33. Takechi-Haraya Y, Goda Y, Sakai-Kato K. Control of Liposomal Penetration into
750 Three-Dimensional Multicellular Tumor Spheroids by Modulating Liposomal
751 Membrane Rigidity. *Molecular Pharmaceutics*. 2017 2017/06/05;14(6):2158-2165. doi:
752 10.1021/acs.molpharmaceut.7b00051.
753
754
755